Improvements in GaSb Homoepitaxial and IMF Solar Cells Grown via Metal-Organic Chemical Vapor Deposition

Emily S. Kessler, Advisor: Dr.Seth Hubbard

ABSTRACT

Current state of the art multijunction solar cells rely on a thick, metamorphic graded buffer from indium gallium arsenide (InGaAs) to gallium arsenide (GaAs) which accounts for nearly 30% of the total device cost. To make these devices more cost effective we propose an alternative, Sb based bottom junction material employing the interfacial misfit (IMF technique), which allows for an immediate lattice constant transition. This technique causes dislocations to preferentially occur in the 90° plane rather than the 60° plane, mitigating dislocations that can degrade solar cell performance. The IMF technique has been heavily studied when grown via molecular beam epitaxy, whereas this work looks to move the technique to a higher throughput technique known as metal-organic chemical vapor deposition (MOCVD). Various parameters for gallium antimonide (GaSb) solar cells, both homoepitaxial and IMF, are studied. For IMF cells both buffer thickness and gallium precursor are studied.

1. INTRODUCTION

With a bandgap of .72 eV, GaSb presents itself as a material that is useful in various applications such as infrared (IR) detectors, light-emitting diodes (LEDs), thermo-photovoltaics, and for the purpose of this work, multi-junction solar cells. Multi-junction solar cells allow for more of the solar spectrum to be collected compared to single junction devices. For a single junction solar cell the Shockley-Queisser Limit is 31% [1], whereas a theoretical 'infinite' junction solar cell has a maximum efficiency of near 87%.

The first attempts at developing triple junction (3J) solar cells used a material stack of Ge(.7 eV)/GaAs(1.4 eV)/InGaP(1.9 eV) [2]. This design has the benefit of being lattice-matched, simplifying the growth. However, due to the bandgap of Ge the design is not current matched, resulting in a loss in open-circuit voltage (V_{OC}) and subsequently a loss in efficiency. The ideal bottom junction bandgap for a 3J cell is 1.0 eV.

The current state-of-the-art 3J solar cell is comprised of InGaAs/GaAs/InGaP with bandgaps of 1.0, 1.4, and 1.9 eV respectively. Despite being current matched, 1.0 eV InGaAs is not lattice matched to GaAs. As a result, a thick, several micron thick stepwise graded buffer is required to incorporate both materials successfully in a solar cell. This buffer is highly growth intensive and can have a threading dislocation density (TDD) on the order of 10^6 cm^{-2}, degrading minority carrier lifetime. Due to the nature of a p-n junctions, such as solar cells, being minority carrier devices, the minority carrier lifetime is a critical to device performance.

An alternative approach is to incorporate $Al_{.30}GaSb$/GaAs/InGaP, which have the optimal bandgaps for a 3J cell, using the interfacial misfit (IMF) array to grow $Al_{.30}GaSb$ (or GaSb for 5J and 6J cells). The IMF growth technique allows interface dislocations to preferentially occur at 90° with a periodicity of GaSb:GaAs being 13:14 lattice sites. Unlike a 60° threading dislocation, the 90° dislocation, or misfit dislocation, will not propagate up into the active layers of the device. This technique has been shown to be capable of producing a TDD of 10^5 cm^{-2}[3].

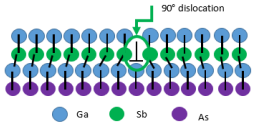

Figure 1: IMF Lattice Structure

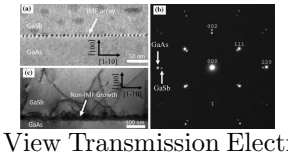

Figure 2: Plan View Transmission Electron Micrograph of IMF and non-IMF Growth

The majority of the literature investigating the IMF growth technique, including its use for photovoltatics, has been done primarily by molecular beam epitaxy (MBE). MBE has the advantage of monolayer growth control, but this has a trade off in growth time, decreasing throughput. Additionally, MBE operates at ultra-high vacuum, making maintenance time-consuming. Metal-organic chemical vapor deposition (MOCVD) is an epitaxial growth method that has not been widely studied for its use of IMF growth. MOCVD has the advantage of higher growth rates and not needing to be operated at ultra-high vacuum pressures.

This work looks to investigate the minority carrier diffusion lengths of both homoepitaxial (GaSb grown on GaSb substrates) and IMF solar cells in order to

determine the optimal cell design for future devices and eventual multijunction cells.

2. METAL-ORGANIC PRECURSOR THEORY

Due to the limited research on the IMF growth technique by MOCVD the optimal metal-organic precursor is not known. TMGa is a simple, well studied precursor. The energy to break the methyl group from the gallium atom is 435 kcal/mol, requiring a fairly high temperature to crack the precursor. This is an issue for goring GaSb because antimony precursors have very low vapor pressures and need to be grown at lower temperatures (less than 600°C)

Figure 3: Trimethlygallium Molecule

Another precursor option is triethylgallium (TEGa). To break the ethyl group off of the gallium atom the energy needed is 410 kcal/mol, less than that needed for methyl groups, resulting in a lower cracking temperature. The additional carbons and hydrogens, however, makes doping of GaSb more difficult to control as carbon is a p-type dopant in III-Vs.

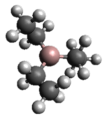

Figure 4: Triethlygallium Molecule

3. MINORITY CARRIER DIFFUSION MODELING

Minority carrier diffusion length is arguably the most important parameter in a solar cell. The minority carrier lifetime determines material quality and dictates how the emitter and base of the solar cell should be designed. Long minority carrier diffusion lengths are desired. The dependence of solar cell parameters such as external quantum efficiency (EQE) and illuminated IV parameters can be determined using the an anylitical drift-diffusion model known as the Hovel Model.

$$J_p = q\int F_0(\lambda)\left\{\frac{L_pF_1(\lambda)+\frac{S_pL_p}{D_p}F_2(\lambda)-F_3(\lambda)\left(\sinh\frac{D_1}{L_p}+\frac{S_pL_p}{D_p}\cosh\frac{d_1}{L_p}\right)}{\left(\cosh\frac{d_1}{L_p}+\frac{S_pL_p}{D_p}\sinh\frac{d_1}{L_p}\right)}\right.$$
$$\left.+\frac{qD_pp_0\left(e^{qV/kT}-1\right)}{L_p}\left\{\frac{\sinh\frac{d_1}{L_p}+\frac{S_pL_p}{D_p}\cosh\frac{d_1}{L_p}}{\cosh\frac{d_1}{L_p}+\frac{S_pL_p}{D_p}\sinh\frac{d_1}{L_p}}\right\}\right.$$

$$F_0(\lambda) = \frac{L_p(1-R_1)\alpha\varphi_0}{\left(1-\alpha^2L_p^2\right)} \quad (2)$$
$$F_1(\lambda) = \alpha \quad (3)$$
$$F_2(\lambda) = 1 \quad (4)$$
$$F_3(\lambda) = e^{-\alpha d_1} \quad (5)$$
$$F_4(\lambda) = \alpha e^{-\alpha d_1}. \quad (6)$$

$$J_n = qe^{-\alpha(W+d_1)}\int F_5(\lambda)\left\{\frac{L_nF_6(\lambda)-\frac{S_nL_n}{D_n}F_7(\lambda)+F_8(\lambda)\left(\sinh\frac{d_2}{L_n}+\frac{S_n}{D}\right.\right.}{\left(\cosh\frac{d_2}{L_n}+\frac{S_nL_n}{D_n}\sinh\frac{d_2}{L_n}\right)}$$
$$\left.+\frac{qD_nn_0\left(e^{qV/kT}-1\right)}{L_n}\left\{\frac{\sinh\frac{d_2}{L_n}+\frac{S_nL_n}{D_n}\cosh\frac{d_2}{L_n}}{\cosh\frac{d_2}{L_n}+\frac{S_nL_n}{D_n}\sinh\frac{d_2}{L_n}}\right\}\right.$$

$$F_5(\lambda) = \frac{L_n(1-R_1)\alpha\varphi_0}{(1-\alpha^2L_n^2)} \quad (8)$$
$$F_6(\lambda) = \alpha e^{-\alpha d_2} \quad (9)$$
$$F_7(\lambda) = e^{-\alpha d_2} \quad (10)$$
$$F_8(\lambda) = 1 \quad (11)$$
$$F_9(\lambda) = \alpha. \quad (12)$$

Where Equations 1 and 7 are the solutions for the hole and electron current respectively. Equation 2-6 and 8-12 are wavelength dependent coefficients. From these values the EQE at various wavelengths can be determined. Using this model GaSb solar cells of varying base thickness were simulated using MATLAB to determine the effect of base minority carrier diffusion length on EQE and illuminated IV. Illuminated IV was using the AM1.5 solar spectrum. Series and shunt resistance was set to values commonly reported in literature, and emitter collection was set to half of the emitter thickness.

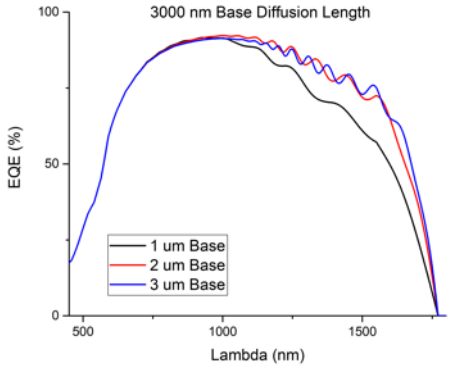

Figure 5: EQE Simulation

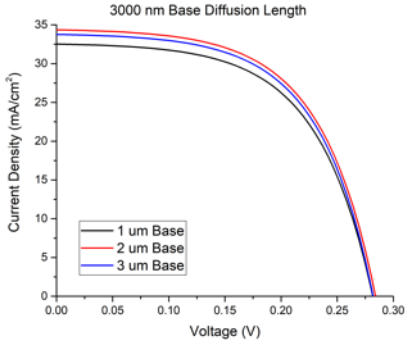

Figure 6: Illuminated IV Simulation

Figure 5 clearly shows base degradation is the base thickness is too thin for the minority carrier diffusion length. The converse is true as well, if minority carrier lifetime is too short and the base thickness is too thick, there is significant base degradation. The decrease in the integrated short circuit current is evident in Figure 6.

4. SOLAR CELL GROWTH AND FABRICATION

All devices were grown on an Aixtron 3x2" Close-Coupled Showerhead MOCVD system at Rochester Institute of Technology in the Semiconductor and Microsystems Fabrication Laboratory. Growth temperature of the GaSb devices was set to 580°C. All devices were grown using trimethylantiomony (TMSb) for the Group V precursor and the V/III ratio was held at 1.2. Homoepitaxial devices using both TMGa and TEGa for GaSb growth are grown. IMF solar cells of varying buffer thicknesses are grown using both precursors and compared. The following device structures were grown:

Figure 7: Homoepitaxial Device Structure

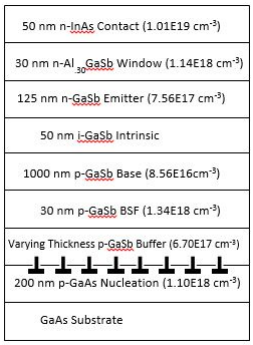

Figure 8: IMF Device Structure

Fabrication of the GaSb solar cells is non-trivial, and requires various time critical steps. Figure 9 shows the process flow followed.

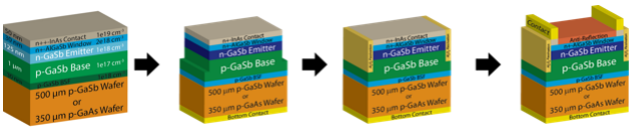

Figure 9: GaSb Fabrication Flow

Devices are first etched in a Citric:HF:H_2O_2 solution that has been shown to improve shunt resistance of the devices by smoothing the device sidewalls. Devices are them passivated using Al_2O_3 deposited via atomic layer deposition (ALD) in an Ultratech Savannah ALD system. This step is highly time critical. The native oxide that forms from GaSb decomposes into elemental Sb, resulting in metal sidewall shunts. As a result, immediately after oxide etched in HCl the devices are immediately loaded into the ALD. The passivation layer is then patterned and the Al_2O_3 is etched in 10:1 HF. Ti/Pt/Au is deposited via electron beam evaporation as the backside sontact. Ti/Au is thermally evaporated for the frontside metal contact and removed in the unwanted regions via a liftoff process. Devices are then

contact etched in a Citric:H_2O_2 solution. All lithography steps are done using a Heidelberg DWL 66+ Direct Write Laser system. Final devices have a radius of 500 μm.

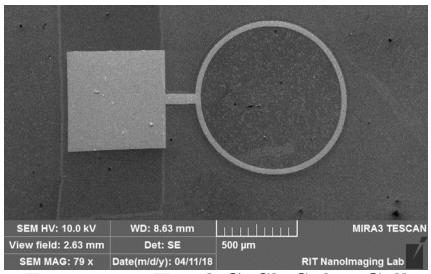

Figure 10: Final GaSb Solar Cell

5. ELECTRICAL RESULTS

5.1 Illuminated IV

Fabricated devices are tested under the AM1.5 solar specturm in order to determine parameters such as open-circuit voltage (V_{OC}), efficiency, and fill factor. AM1.5 Illuminated IV is conducted using a TSS Solar Simulator.

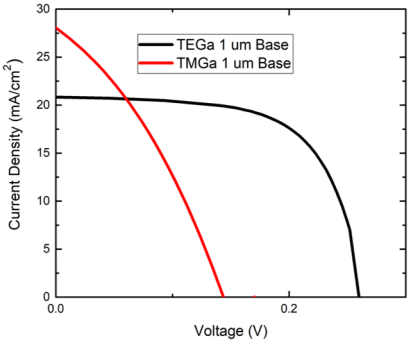

Figure 11: Homoepitaxial Illuminated IV

From Figure 11 it is clear that the TEGa homoepitaxial device is superior to the TMGa sample in virtually all parameters. The TMGa device shows heavy shunting, which may be due to issues in fabrication. Extracted illuminated IV parameters are:

Table 1: Homoepitaxial Illuminated IV Results

	V_{OC} (mV)	Fill Factor (%)	Efficiency (%)
TEGa	269	53	3.34
TMGa	145	34	1.37

The open circuit voltage of the TEGa device is approaching the simulated goal multijunction open circuit voltage of 360 mV. The fill factor of the TMGa device indicates issues that occurred during fabrication, likely due to the passivation step.

IMF devices of varying buffer thicknesses are also tested using the same setup. In Figure 12 the open circuit voltage versus buffer thickness for both TMGa and TEGa devices is plotted.

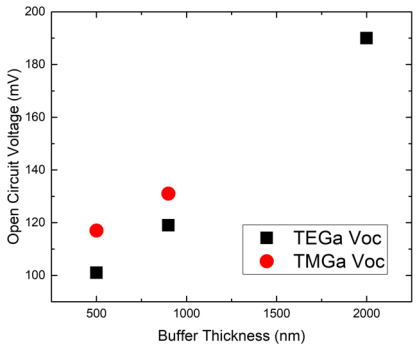

Figure 12: Buffer Thickness vs. Open Circuit Voltage

It is clear from Figure 12 that as buffer thickness increases, open circuit voltage increases. This is likely due to threading dislocations terminating as the buffer is grown thicker, resulting in fewer defects in the active region of the device. The 2000 nm device using TEGa demonstrates an open circuit voltage approaching 200 mV, better than that of the TMGa homoepitaxial device. This suggests that this device could be utilized in a multijunction solar cell, especially under concentration.

5.2 External Quantum Efficiency

External quantum efficiency is taken for all devices from 500 nm to 1800 nm in scan steps of 10 nm. Device measurements are

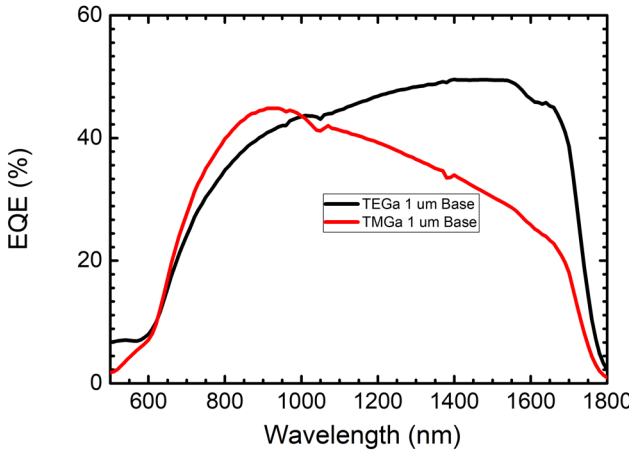

Figure 13: Homoepitaxial Quantum Efficiency

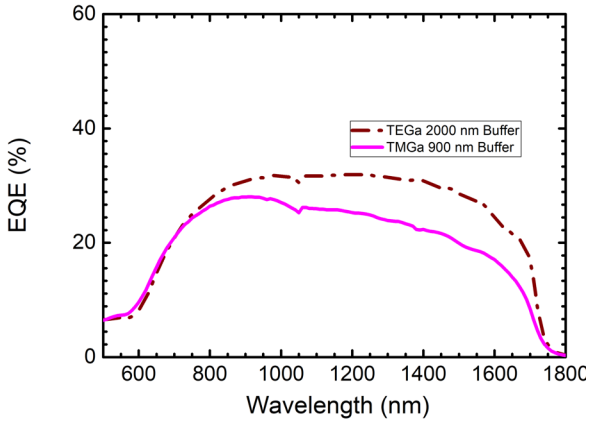

Figure 14: IMF Quantum Efficiency

In both the homoepitaxial and IMF devices the base region of the device is degraded when using TMGa. In the emitter region, however, the homoepitaxial device using TEGa displays slightly better performance. This is confirmed by fitting the quantum efficiency and determining the minority carrier diffusion length in each region using the Hovel model outlined in Section 3.

Table 2: Homoepitaxial Extracted Minority Carrier Diffusion Lengths

	L_E (nm)	L_B (nm)	S_E (cm/s)	S_B (cm/s)
TEGa	75	>>3x base thickness	$>>10^6$	$<<10^6$
TMGa	196	600	$>>10^6$	$<<10^6$

Table 3: IMF Extracted Minority Carrier Diffusion Lengths

	L_E (nm)	L_B (nm)	S_E (cm/s)	S_B (cm/s)
TEGa 2000 nm Buffer	20	693	$>>10^6$	$>>10^6$
TMGa 900 nm Buffer	14	310	$>>10^6$	$>>10^6$

TEGa demonstrates superior minority carrier lifetime in the base region universally. In both the homoepitaxial and IMF devices the front surface recombination velocity (S_E) is set very high. This is due to the poor interface between the AlGaSb window and the GaSb emitter, resulting in a loss of carriers that are recombining at the interface and not making it to the junction. In the IMF devices the rear surface recombination velocity is also set very high. This is likely due to a graded defect density in the IMF devices, with a higher dislocation density closer to the base region of the device.

6. CONCLUSION

GaSb homoepitaxial and IMF solar cells are grown, fabricated, and tested. Both TEGa and TMGa is investigated to determine which metal-organic precursor is more favorable. From both the illuminated IV and EQE measurements it is clear that TEGa is the preferred precursor. Future work would be the investigation of the AlGaSb/GaSb interface to accurately determine the surface recombination velocity. Additionally, the IMF interface can be further optimized to decrease defects at the interface and further reduce the necessary buffer thickness.

7. REFERENCES

1 . Karam, "40% efficient metamorphic GaInP/GaInAs/Ge multijunction solar cells", Appl. Phys. Lett., vol. 90, no. 18, p. 183516, 2007

2 . A. Jallipalli, G. Balakrishnan, S. Huang, T. Rotter, K. Nunna, B. Liang, L. Dawson and D. Huffaker, "Structural Analysis of Highly Relaxed GaSb Grown on GaAs Substrates with Periodic Interfacial Array of 90 degree Misfit Dislocations", Nanoscale Res Lett, vol. 4, no. 12, pp. 1458-1462, 2009.

3 . Mohammedy, F. and Jamal Deen, M. (2009). Growth and fabrication issues of GaSb-based detectors. Journal of Materials Science: Materials in Electronics, 20(11), pp.1039-1058.

4 . Shockley, William and Hans J. Queisser. "Detailed Balance Limit Of Efficiency Of P-N Junction Solar Cells". J. Appl. Phys. 32.3 (1961): 510. Web. 27 July 2016.

5 . R. King, D. Law, K. Edmondson, C. Fetzer, G. Kinsey, H. Yoon, R. Sherif and N.